Active surface transport of metabotropic glutamate receptors through binding to microtubules and actin flow

Arnauld Sergé‡, Lawrence Fourgeaud, Agnès Hémar and Daniel Choquet*

Physiologie Cellulaire de la Synapse, CNRS UMR 5091, Institut François Magendie, rue Camille saint Saëns, 33077 Bordeaux, Cedex, France
*Author for correspondence (e-mail: dchoquet@u-bordeaux2.fr)
‡Present address: Centre d'Immunologie de Marseille-Luminy, Université de la Méditerranée - Case 906, 13009 Marseille, France

Accepted 6 August 2003
Journal of Cell Science 116, 5015-5022 © 2003 The Company of Biologists Ltd
doi:10.1242/jcs.00822

Summary

Receptors for neurotransmitters are concentrated and stabilized at given sites such as synapses through interactions with scaffolding proteins and cytoskeletal elements. The transport of receptors first involves directed vesicular trafficking of intracellularly stored receptors followed by their targeting to the plasma membrane. Once expressed at the cell surface, receptors are thought to reach their final location by random Brownian diffusion in the plasma membrane plane. Here, we investigate whether the metabotropic glutamate receptor mGluR5 can also be transported actively on the cell surface. We used single particle tracking to follow mGluR5 movement in real time at the surface of neuronal growth cones or fibroblast lamellipodia, both of which bear a particularly active cytoskeleton. We found that after a certain lag time mGluR5 undergoes directed rearward transport, which depends on actin flow. On actin depolymerization, directed movement was suppressed, but receptors still bound to a rigid structure. By contrast, receptor transport and immobilization was fully suppressed by microtubule depolymerization but favored by microtubule stabilization. Furthermore, mGluR5 could be immunoprecipitated with tubulin from rat brains, confirming the ability of mGluR5 to bind to microtubules. We propose that mGluR5 can be transported on the cell surface through actin-mediated retrograde transport of microtubules. This process may play a role in receptor targeting and organization during synapse formation or during glutamate-mediated growth cone chemotaxis.

Movie available online

Key words: mGluR5, Transport, Microtubules, Actin flow, Single particle tracking

Introduction

Receptors for neurotransmitters usually have a precise subcellular distribution in neurons and are mostly concentrated at synaptic sites. This is necessary for their correct function in synaptic transmission. Their localization is maintained by their anchorage to rigid structures such as scaffolding proteins, cytoskeletal elements, the extracellular matrix or cell adhesion molecules. Otherwise, they would rapidly be distributed evenly in the whole cell membrane. Indeed, a transmembrane protein not bound to a rigid structure, free to move in the plane of the membrane, diffuses at a rate of around 0.1 $\mu m^2/s$ (Kusumi et al., 1993; Sergé et al., 2002).

Receptors are also found dispersed in the extrasynaptic membrane. We (Borgdorff and Choquet, 2002; Meier et al., 2001; Sergé et al., 2002) and others (Akaaboune et al., 1999; Salpeter and Loring, 1985; Tovar and Westbrook, 2002; Zhou et al., 2001) have suggested that receptors can alternate between synaptic and extrasynaptic locations through lateral diffusion in the plane of the membrane. Receptors are, in fact, in a dynamic equilibrium between a diffuse mobile state and an immobile stabilized state due to binding to scaffold elements. For example, both ionotropic AMPA and glycine receptors, as well as metabotropic glutamate receptor 5 (mGluR5), constantly alternate between immobile and freely mobile states (Borgdorff and Choquet, 2002; Meier et al., 2001; Sergé et al., 2002). The residence time of a given receptor in the stabilized state is greatly increased by the presence of its associated scaffold protein. However, the clustering of receptors by scaffold proteins is not sufficient for their immobilization. Indeed, we found that clustered receptors exhibit a highly variable degree of mobility in the plane of neuronal membranes. We attributed this variability to different degrees of binding to rigid cytoskeletal structures (Sergé et al., 2002).

During synapse formation or plasticity, the targeting of receptors to specific synaptic domains is thought to result from the association of both this process of random diffusion-trap at the cell surface and the local exocytosis of receptors following trafficking by intracellular transport mechanisms (Passafaro et al., 2001; Rosenberg et al., 2001). Directed transport of neurotransmitter receptors have so far only been observed during intracellular trafficking. Ionotropic AMPA (Kim and Lisman, 2001; Setou et al., 2002) and NMDA (Setou et al., 2000) receptors are transported from the cell body to neurites through binding to microtubule-linked motors (kinesins and dyneins).

We wanted to determine whether neurotransmitter receptors can also be actively transported on the neuronal surface. In our

previous studies performed on neurites, we very seldom observed directed movement of receptors. However, some neuronal regions, such as growth cones or spines, display a highly dynamic cytoskeleton (Matus, 2000; Smith, 1988), and receptors can be bound to cytoskeletal elements (for example, see Allison et al., 1998; Kirsch et al., 1991). We thus investigated whether receptors could be transported through cytoskeleton remodeling. We chose mGluR5, a member of group I mGluRs, as model receptors because they are expressed early during neuronal development (Conn and Pin, 1997; Romano et al., 1996), can be expressed on growth cones (Kreimborg et al., 2001) and could play a role in regulating neuronal chemotaxis (Behar et al., 1999) or migration. Receptors in this group can bind tubulin (Ciruela and McIlhinney, 2001; Ciruela et al., 1999). In mature neurons, they are located in an annulus surrounding the postsynaptic density (Lujan et al., 1997; Nusser et al., 1994; Vidnyanszky et al., 1994), as well as in the extrasynaptic and, in some structures, presynaptic membranes (Romano et al., 1995; van den Pol et al., 1995). We previously showed that mGluR5 displays variable degrees of mobility in neurites – it is downregulated by its associated intracellular scaffolding protein homer and upregulated by agonist treatment (Sergé et al., 2002).

Growth cones are among the most active neuronal regions in terms of cytoskeleton dynamics. Their cytoskeletal structure and organization is homologous to that of the lamellipodia of other migrating cells such as fibroblasts. In both structures, actin is polymerizing at the leading edge, producing a protrusive force on the front membrane. At the same time, actin is depolymerizing at the base of the structure. These two processes combined with the action of motors (Lin et al., 1996) produce a global movement of the gel of polymerized actin that fills the cytosol of the structure and is at the origin of cell movement. The whole process is called actin flow (reviewed by Pantaloni et al., 2001). This rearward actin movement is able to transport surface glycoproteins at rates around 1 μm/min, as shown using tracking of the movement of receptor bound to single particles (Sheetz et al., 1989). Such transport has been shown for several adhesion proteins involved in cell migration such as integrins (Felsenfeld et al., 1996; Grabham et al., 2000), neuron-glia related cell-adhesion molecule (NrCAM) (Faivre-Sarrailh et al., 1999), aplysia cell-adhesion molecule (ApCAM) (Thompson et al., 1996) and cadherins (Lambert et al., 2002), but it has never been investigated for neurotransmitter receptors. We used single particle tracking (SPT) in neuronal growth cones and fibroblast lamellipodia to show that mGluR5 can be retrogradely transported by actin flow. This transport is probably due to mGluR5 binding to microtubules, which are then themselves transported by actin.

Materials and Methods

Cultures, constructs and transfection procedures

NIH 3T3 cells were grown in Dulbecco's modified Eagle's medium without phenol red and with 20 mM Hepes pH 7.2, 10% calf serum, 2 mM penicillin/streptomycin/glutamax at 37°C and 5% CO_2. Hippocampal neurons were obtained from E18 rat embryos, and cultured as described (Hémar et al., 1997). All cells were grown on glass coverslips. The myc-tagged mGluR5 has been previously described (Sergé et al., 2002). The mGluR5 cytoplasmic deletion mutant, mGluR5-delC-myc (N887stop) was provided by J. P. Pin (CCIPE, Montpellier, France) (Mary et al., 1998). 3T3 cell transfections were performed in subconfluent (60-70%) cultures using Fugen (Roche Diagnostics). Neurons were transfected 2 to 7 days after plating using effecten (Qiagen). Both protocols were performed following the manufacturer's indications. Transient expression was allowed for 24 to 48 hours at 37°C and 5% CO_2.

Video microscopy and optical trapping

Experiments and data analysis were performed essentially as described (Meier et al., 2001; Sergé et al., 2002). Briefly, cultured cells were mounted in culture medium in a chamber between two coverslips. The chamber was installed on an IX-70 inverted Olympus microscope heated at 37°C with an air blower (Word Precision Instruments). Cells were visualized under red illumination and differential interference contrast (DIC) through a 100× Planapo objective (n.a. 1.4) on a C2400 camera (Hamamatsu). Images were treated by background substraction and contrast enhancement online. An optical trap was formed in the plane of focus with the beam of a Ti: sapphire laser (Spectra-Physics) tuned at 800 nm, 200 mW. Latex beads of 1 or 0.5 μm in diameter (Polysciences) coated with anti-myc antibodies were manipulated with the optical trap, and maintained for 5 seconds in contact with the surface of the transfected cell to allow their attachment to the myc-tagged receptors. On release of the trap, the beads remaining in the plane of focus were scored as attached and video images recorded on a VCR for later analysis. 46% and 14% of the beads attached to transfected and nontransfected cells, respectively, indicating a good specificity of binding. Variations in the radius of the beads had no significant effect on the reported results. Transfected cells were identified under epifluorescence by the presence of green fluorescent protein (GFP) co-transfected with the myc-tagged receptor. For drug application, the 100 μl chamber was perfused with 500 μl of medium containing either 1 μM cytochalasin D, 10 μM demecolcine, 1 μM nocodazol or 10 μM taxol (all products from Sigma).

Bead tracking and data analysis

Video images were digitized at 25 Hz with a DVR (Imasys) and bead positions were followed using homemade software (Choquet et al., 1997) with an accuracy of 5-10 nm. The mean squared displacement (MSD) function was computed as described by Sergé et al. (Sergé et al., 2002).

The relative deviation from Brownian diffusion is computed as described by Kusumi et al. (Kusumi et al., 1993) by the ratio between the MSD calculated at 10% of the total time and the extrapolated value that would be found for a linear MSD, computed from the slope at the origin. This relative deviation is equal to 1 for Brownian movements and above 1 for directed movements.

$$RD = \frac{MSD(T/10)}{4.D.T/10},$$

where T is the total time of the recorded trajectory and D the diffusion coefficient computed from the initial slope of the MSD function versus time by linear fitting over the second, third and fourth data points.

Immunoprecipitation and western blot analysis

After dissection, hippocampi from Wistar rats (4-8 weeks) were homogenized on ice in buffer containing 25 mM hepes, pH 7.4, 150 mM NaCl and a mix of protease inhibitors: pepstatin 10 μg/ml, leupeptin 10 μg/ml, aprotinin 10 μg/ml and pefabloc 20 μg/ml). For two hippocampi, homogenization was done in 750 μl of homogenization buffer. The homogenate was solubilized by mixing in 1:1 ratio with the solubilization buffer (homogenization buffer plus 2%

triton X-100). After 20 minutes on ice, the lysate was spun at 8000 ***g*** for 10 minutes. One milligram of total hippocampal lysate was diluted in 1 ml in lysis buffer (homogenization buffer plus 1% triton X-100) and pre-cleared during 30 minutes with 50 µl of protein A agarose beads (APB). Then the lysate was incubated 1 hour with a specific antibody: anti-mGluR5 (4 µg, Upstate biotechnology #06-451) or anti-β tubulin (5 µl, clone TUB 2.1 SIGMA). The complex was collected overnight on 50 µl protein A agarose beads. The immunoprecipitate was eluted by boiling in 4× SDS gel-loading buffer and run in 7% SDS-PAGE. Fifty micrograms of the lysate were run in the same gel. After electrophoretical transfer, membranes were blocked in phosphate buffer saline (PBS), 5% milk and washed in PBS, 0.1% tween 20 before incubation with primary antibodies: anti-mGluR5 (0.8 µg/ml) or anti-transferrin receptor (1 µg/ml, H68.4, SIGMA) for 1 hour in PBS, 0.1% tween-20, 1% milk. Immunoreactive bands were detected with an appropriate secondary antibody conjugated to horseradish peroxidase (HRP) (Fab'2 anti-rabbit 1/3000 and anti-mouse 1/3000 from P.A.R.I.S.). Membranes were developed with enhanced chemiluminescence (APB) and exposed to autoradiographic film (biomax MR, Eastman Kodak) to detect HRP.

Results

mGluR5 is transported rearward on cell lamellipodia

We performed SPT experiments on cultured hippocampal neurons and fibroblasts transfected with the cDNA encoding mGluR5a tagged at its extracellular N-terminus with a c-myc epitope (mGluR5-myc). This allowed coupling of micrometric latex beads covered with myc antibodies to the tagged receptors. Beads were manipulated with optical tweezers made of an infrared laser beam focused by the objective of the microscope. For each record, a bead was held with the laser tweezers in contact with a transfected cell to allow coupling to mGluR5-myc, and then released from the tweezers. Beads remaining in the plane of focus were scored as attached and their movement, reflecting that of the underlying receptors, was then followed by video microscopy.

In control conditions, both in neuronal growth cones and in fibroblast lamellipodia, after release of the tweezers, beads initially underwent free rapid Brownian diffusion on the lamellipodium. This is apparent from the trajectories of mGluR5-coupled beads superimposed on DIC pictures of the recorded cells (Fig. 1A,B). Beads then often switched to a directed retrograde movement towards the cell body, characterized by a low diffusion coefficient and a directed motion. This transition was clearly apparent on plots of the diffusion coefficient versus time (Fig. 1D,E) and we termed it anchorage of the receptors, as they were no longer freely diffusing (see Movie 1, showing a representative mGluR5-coupled bead movement on a fibroblast lamellipodium, http://jcs.biologists.org/supplemental/). To detect the time of occurrence of this transition accurately, we used a mathematical function corresponding to the ratio between the mean diffusion during the 20 seconds before and after a given timepoint. This coefficient is close to 1 during phases bearing a constant average diffusion, and is elevated at transition points where the diffusion coefficient decreases. A detectable switch (coefficient above 5) occurred more frequently in fibroblast (85% of trajectories, *n*=20 beads) than in neuronal growth cones (23% of trajectories, *n*=13). Anchorage was less frequent on neurites (10% of trajectories, *n*=58) and not associated with directed movement.

Because the fibroblast lamellipodia is a well-established model for actin flow and these cells are transfected more easily than neurons, we performed the subsequent quantitative analysis in fibroblasts. In these cells, the mean time for anchorage to occur after release of the bead from the tweezers was 20±5 seconds (*n*=20) (52 seconds in the example depicted in Fig. 1A,D,G). In contrast to the stabilization of the receptors induced by homer described previously (Sergé et al., 2002), the

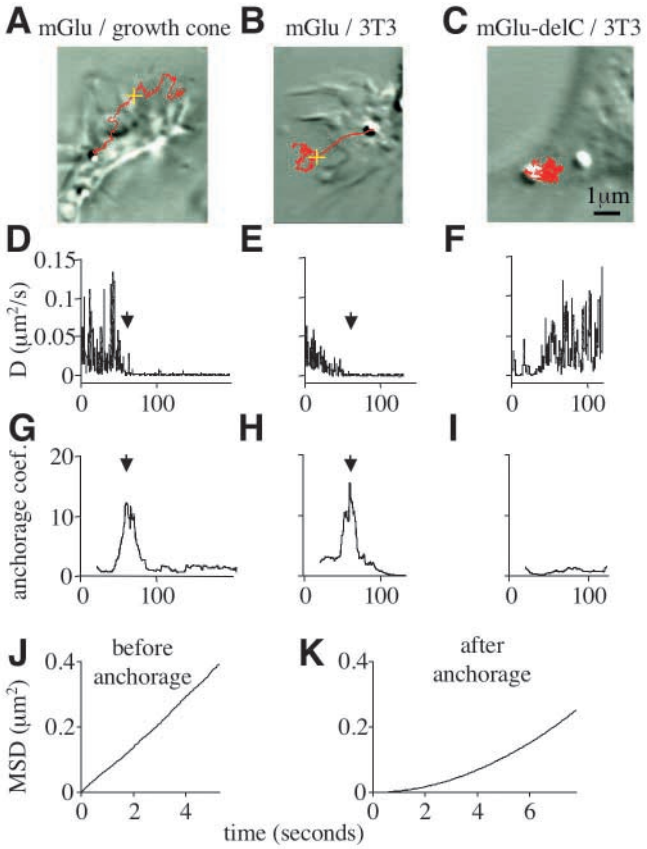

Fig. 1. mGluR5 displays anchorage through its C-terminus. Typical trajectories (red lines) on a hippocampal neuron growth cone (A) and on fibroblast lamellipodium (B,C) of latex beads coupled to mGluR5-myc (A,B) or a C-terminal deletion mutant (C) superimposed on a DIC image of the cell. Trajectories in A and B present anchorage as an irreversible transition between Brownian diffusion and linear retrograde movement. The point of the trajectory corresponding to the transition is depicted by a yellow cross. Recording time, 125-200 seconds; sampling time, 25 images/second. (D-F) Plots of diffusion versus time corresponding to the trajectories in (A-C). For each timepoint, the diffusion coefficient was computed from the slope of the MSD calculated for 40 points. Note the sudden drop in diffusion values in D and E, depicted by arrows and corresponding to the yellow crosses in A and B. (G-I) Plots of the anchorage coefficient versus time corresponding to the trajectories in (A-C). For each timepoint, the anchorage coefficient was computed as the ratio between the mean diffusion during the 20 seconds before and after that timepoint. The maximum of this coefficient (black arrows) thus corresponds to the drop in diffusion values depicted by the corresponding arrows in D and E, whereas the coefficient remains low during all the recording time for mGluR5-DelC (F). (J,K) Plots of the MSD versus time for the control trajectory recorded on fibroblast depicted in B, computed before and after anchorage. Note the linearity of the MSD before anchorage, and the positive curvature displayed after.

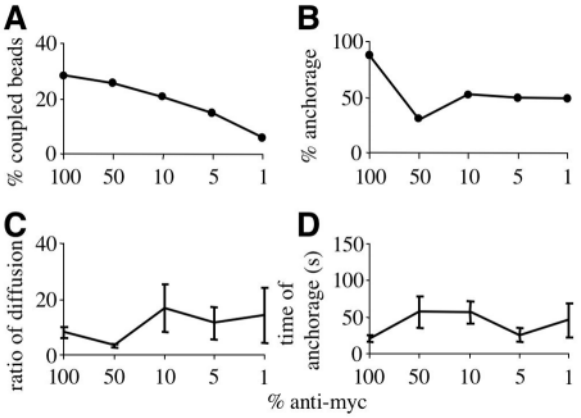

Fig. 2. Anchoring is not induced by cross-linking of receptors by the bead. (A) Plot of the percentage of beads efficiently attached to transfected cells. In all graphs of this figure, the anti-myc antibody coupled to the bead was diluted with another anti-HA antibody, unable to bind to the tagged receptors, in the given proportions (percentage of anti-myc relative to total amount of antibodies coupled to the bead, as depicted on the x-axis). (B) Plot of the percentage of trajectories displaying anchorage for various dilutions of the anti-myc antibody. (C) Plot of the mean ratio of the diffusion coefficients computed before and after anchorage, for various dilutions of the anti-myc antibody. In all figures, values are given with s.e.m. (D) Plot of the time for anchorage for various dilutions of the anti-myc antibody. Note that only the percentage of beads efficiently coupled to transfected cells is diminishing with dilution of the anti-myc antibody, whereas the percentage of trajectories displaying anchorage, the mean ratio of the diffusion coefficients computed before and after anchorage, and the time of anchorage remain almost constant. This shows that anchorage does not rely on aggregation of receptors by the beads.

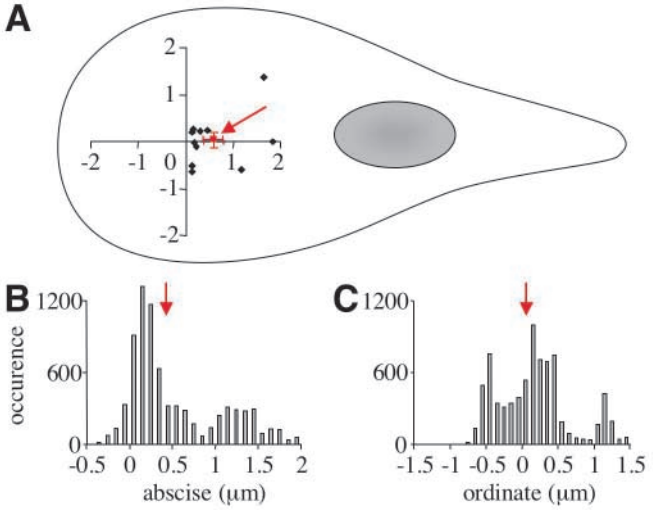

Fig. 3. Spatial aspect of anchorage. (A) Plot of the spatial position of the anchorage points (diamonds), corresponding to the maximum of the anchorage coefficient function and depicted by the yellow cross on trajectories, as illustrated in Fig. 1, for control trajectories recorded on fibroblasts. Trajectories were aligned by rotation with the cell body along the positive x-axis (as measured by the direction of the linear movement after anchorage), with the initial point of the trajectory assigned to the origin of the plot. Note that the mean position (square, indicated by the arrow) is already situated along the positive abscises. Trajectories anchored from the beginning were discarded for this plot. (B,C) Histograms of the abscises and ordinates of the receptors positions during the first, diffusive phase. Note that the mean abscise is positive whereas the ordinates are centered on 0 (arrows).

anchorage of the receptors on growth cones was irreversible in the time frame of our experiments (200 seconds). Indeed, we only observed a transition from a low to a high diffusion phase in one out of 91 trajectories.

To gain insight into the characteristics of the receptor movements in the different phases, we computed the mean squared displacement (MSD) versus time before and after the switch point (Fig. 1J,K). On the first part of the trajectory (depicted in Fig. 1B), the MSD versus time is linear, as expected for a Brownian motion. In the second part, the MSD is parabolic, as expected for a linear movement, and displays a low diffusion coefficient, which is indicative of binding to a rigid structure moving in a directed manner. The relative deviation from Brownian diffusion for movements of mGluR5-myc is equal to 0.5±0.03 (n=15) for the first part of the trajectories, and reaches 4.9±0.9 (n=18, P<0.001, Student's t-test) for the second part. This confirms that receptors undergo directed movement when they are anchored.

As a control and to investigate which receptor domain is involved in anchorage, we studied the movement of a mutant of the receptor deleted of most of its intracellular C-terminal domain. mGluR5-delC displays no anchorage, as illustrated in Fig. 1C,F,I (n=5), and quantified in Fig. 5A,B. The mean global diffusion of the deletion mutant was greater than that of the full-length receptor (D=14±8 10^{-3} and 4±1 10^{-3} μm^2/s), thus indicating the involvement of the intracellular tail in the anchorage process.

Extensive receptor aggregation induced by the multivalence of the antibody-coated bead could potentially be a trigger for receptor binding to cytoskeleton, as previously observed for some adhesion proteins (Faivre-Sarrailh et al., 1999; Felsenfeld et al., 1996; Grabham et al., 2000; Lambert et al., 2002). We thus studied the influence on receptor movement or the extent of receptor aggregation by diluting the antibody concentration on the bead surface. This affected only the percentage of beads that could be efficiently attached to transfected cells (Fig. 2A). The percentage of beads that anchored, the ratio of diffusion between the two phases of movement and the time for anchorage to occur were not significantly affected by dilutions of the anti-myc antibody covering the bead by factors of 2, 10, 20 or 100 (n=10, 15, 12 and 6, respectively; Fig. 2B-D).

We then analyzed the spatial position of the anchorage point for trajectories recorded on fibroblasts (Fig. 3A). On average, this point is located at 0.6 μm from the origin along the x-axis (Fig. 3A). Furthermore, the histogram of all x-axis values of points of the diffusing phase of the trajectories (Fig. 3B) is centered on a positive mean value of 0.4 μm, whereas the histogram of the y-axis values is centered on 0 (Fig. 3C). This indicates that during the first part of Brownian diffusion, the trajectory is in fact skewed toward the positive abscises and suggests that the point where anchorage occurs is reached by random movement.

During the second phase, both the direction of the linear movement towards the cell body and the mean speed of the

receptors (v=2.3±0.3 μm/min, *n*=20, in fibroblast and v=1.0±0.7 μm/min, *n*=3, in neuronal growth cones) are fully compatible with the reported direction and speed of actin flow in growth cones (ranging from 1 to 4.6 μm/min) (Danuser and Oldenbourg, 2000; Schmidt et al., 1995). We thus interpreted the transition between the two phases as an anchorage of the receptor to a rigid structure that would be dragged by the actin flow, after an initial period of free diffusion.

Characterization of the binding structure

To characterize the rigid structure to which the receptors are anchored, we performed a pharmacological study using various drugs against different components of the cytoskeleton. Depolymerization of actin by 1 μM cytochalasin suppressed the retrograde movement, as expected for an involvement of actin flow. However, the second phase of reduced mobility remained (Fig. 4A,E): during the second phase, the receptor movement was no longer rearward toward the cell body; instead, the receptor kept on diffusing, but with a smaller diffusion coefficient (Fig. 4E). In the presence of this drug, the mean global MSD was linear, further confirming the absence of retrograde movement (Fig. 4I; *n*=16).

Depolymerization of microtubules by either 10 μM demecolcine or 1 μM nocodazol suppressed the second phase of reduced mobility. In the presence of these drugs, the receptor was highly diffusing throughout the experiment (200 seconds on average), without a significant decrease in diffusion rate with time (Fig. 4B,C,F,G). Furthermore, the mean MSD was almost linear, confirming the diffusive nature of the movement (Fig. 4J; *n*=8, data not shown for demecolcine, which led to similar results as for nocodazol). Diffusion was higher than in controls conditions or in the presence of cytochalasin, as can be seen on the initial slope of the MSD (Fig. 4I, inset, to compare with the initial slope in the presence of cytochalasin, Fig. 4J, inset).

To further investigate the role of microtubules in mGluR5 anchorage, we used taxol, which stabilizes microtubules. In the presence of 10 μM taxol, trajectories still displayed a directed movement (Fig. 4D,H). The mean delay for anchorage to occur in the presence of taxol was 19±9 seconds (*n*=18), a value similar to that observed in control conditions (20±5 seconds, *n*=20), but more trajectories were anchored from the beginning of the record with taxol (44%) than in control (32%). More significantly, the speed of rearward movement, calculated on the mean MSD, was greater (2.9 μm/min) than in control conditions (1.8 μm/min).

These results are summarized in Fig. 5, which shows the mean diffusion and relative deviation from Brownian motion in the different conditions. Diffusion was increased for the C-terminal deletion mutant as well as for the full-length receptor in the presence of drugs that depolymerize either actin (cytochalasin) or microtubules (demecolcine, *n*=10, and nocodazol). However, diffusion was of the same order of magnitude than in control conditions in the presence of a drug that stabilizes microtubules (taxol). Likewise, the relative deviation was close to 1, as expected for pure diffusion, for the C-terminal deletion mutant as well as in the presence of cytochalasin, demecolcine and nocodazol. By contrast, the relative deviation was significantly above 1, as expected for linear movements of anchored particles dragged by the actin flux, in control conditions and in the presence of taxol. Altogether, these data suggest that in control conditions the receptor anchors to microtubules, which in turn are transported rearward by actin flow.

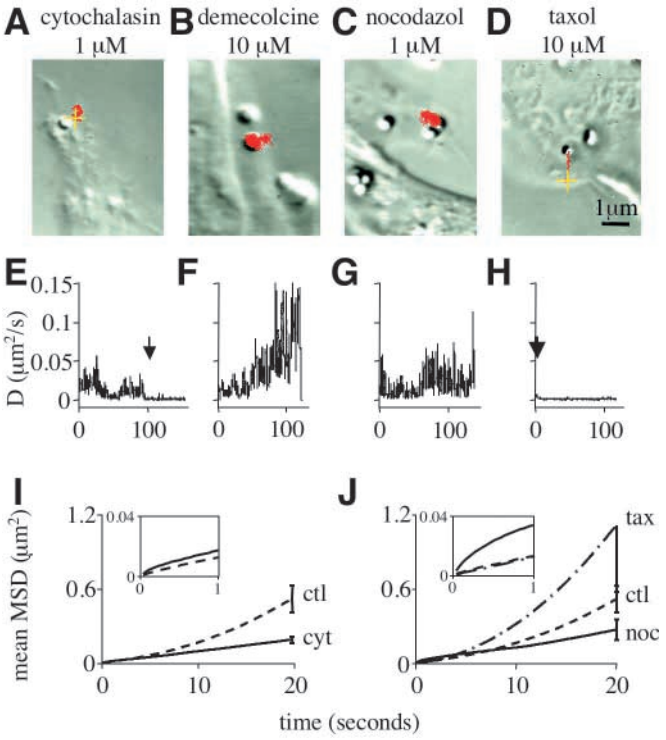

Fig. 4. Pharmacological characterization of the anchoring structure. (A-D) Typical trajectories (red) on fibroblast lamellipodium of latex beads coupled to mGluR5-myc superimposed on a DIC picture of the cell, in the presence of drugs that affect the cytoskeleton. (A) Trajectory in the presence of 1 μM cytochalasin, which depolymerizes actin. (B,C) Trajectories in the presence of 10 μM demecolcine or 1 μM nocodazol, which depolymerize microtubules. (D) Trajectory in the presence of 10 μM taxol, which stabilizes microtubules. Anchorage points are depicted by yellow crosses (A,D). Note that anchorage remains when actin is depolymerized (A) or when microtubule polymerization is favored (D), and is abolished when microtubules are depolymerized (B,C). (E-H) Corresponding diffusion versus time plots. Note the sudden drop in diffusion values in E and the low values recorded from the beginning in H (arrows), corresponding to the yellow crosses in A and D, respectively. (I-J) plots of the mean MSD versus time for control trajectories recorded on fibroblasts in control conditions and in the presence of drugs that affect actin (I) or microtubules (J). Note that the positive curvature of the mean MSD in the presence of taxol (tax) is even higher than in control (ctl), whereas the mean MSD is lower and linear with time in the presence of cytochalasin (cyt) and nocodazol (noc) ($P<0.01$ and $P<0.05$, respectively). Insets: blowup of the MSD versus time plots around the origin; J shows the increase in diffusion under nocodazol.

To confirm biochemically the interaction of mGluR5 and microtubules, we looked for co-immunoprecipitation of mGluR5 with β-tubulin. Fig. 6 shows that mGluR5 was detected by western blot in an immunoprecipitate of β-tubulin from extracts of isolated rat hippocampi (lane b). This interaction was specific as the transferrin receptor failed to be precipitated under the same conditions (Fig. 6, lane c). This

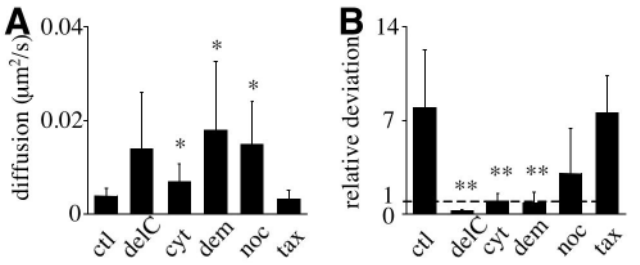

Fig. 5. (A,B) Histogram of the mean diffusion and mean relative deviation from Brownian diffusion in control conditions (ctl), for the C-terminal deletion variant (delC) or in the presence of drugs affecting the cytoskeleton. Note that diffusion is increased in the presence of cytochalasin (cyt), demecolcine (dem) or nocodazol (noc) (**P*<0.05) and relative deviation is decreased for the C-terminal deletion variant or in the presence of cytochalasin or demecolcine (***P*<0.01).

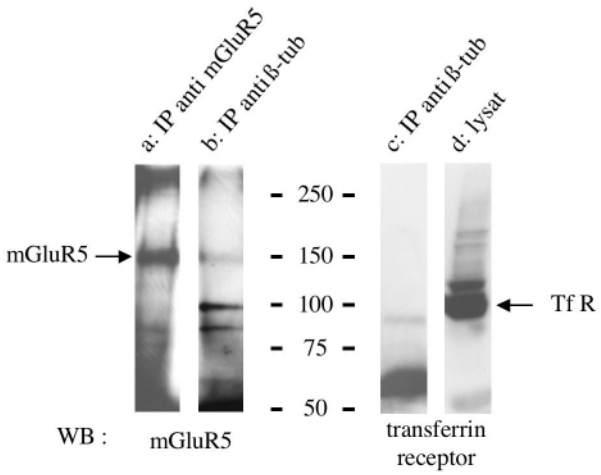

Fig. 6. mGluR5 is immunoprecipitated with β-tubulin in rat hippocampal lysates. Hippocampal lysates were immunoprecipitated with anti-mGluR5 (lane a) or anti-β-tubulin (lanes b and c) as indicated. Immunoprecipitates and lysate (lane d) were immunoblotted as indicated for mGluR5 (lanes a and b) or transferrin receptor proteins (TfR) (lanes c and d, negative control). IP, immunoprecipitate; WB, western blot.

shows by an independent method that mGluR5 and tubulin are associated in a complex.

Discussion

In this paper we have used single particle tracking to characterize the movement of mGluR5 in neuronal and fibroblastic lamellipodia, a cell region with an active cytoskeleton. Anchorage is more than twice as frequent in growth cones than in neurites. Most receptor trajectories showed an initial diffusive part followed by a directed movement towards the cell body due to binding of mGluR5 to a moving rigid structure. This structure was identified as microtubules both by pharmacology and biochemistry. Disrupting microtubules abolished the anchoring of receptors, whereas stabilizing microtubules favored it, and mGluR5 could be co-immunoprecipitated with tubulin. Furthermore, depolymerizing actin abolished the retrograde movement, but not the anchoring. We therefore propose a model in which receptors are initially freely diffusive in the lamellipodium membrane and then, after binding to a microtubule, are drawn back towards the cell body due to cross-linking between the bound microtubule and the actin flow. Measured speeds of this linear movement are fully compatible with this interpretation. Furthermore, the speed of receptor rearward movement is increased by rigidification of the microtubules. This is likely to arise from a more robust coupling between microtubules and the actin gel. Most importantly, retrograde movement of microtubules powered by actin flow has been directly visualized previously using tubulin-rhodamine and video-microscopy (Waterman-Storer and Salmon, 1997).

That receptors initially diffuse before undergoing directed movement could have different origins. It could arise from a time-dependent recruitment of receptors under the bead, a time-dependent activation of the capacity to bind to microtubules, to a space-dependent encounter of a binding site, i.e. a microtubule. Several arguments prompt us to favor the latter hypothesis. Time-dependent recruitment of receptors under the bead as the basis for the decrease in receptor diffusion is unlikely as receptor anchoring is not dependent on the amount of antibodies at the surface of the bead, which could be diluted up to 100 times with no detectable effect. Furthermore, theoretical and experimental studies have shown that diffusion of an aggregate of receptors in a membrane only varies with the logarithm of its size (Kucik et al., 1999; Saffman and Delbruck, 1975). Because specific bead binding to cells was lost for antibody dilutions on the bead surface below 1/100, we estimate that fewer than 100 receptors are bound to each bead. Cross-linking of the receptors by the bead could potentially be a trigger for anchoring to the cytoskeleton. Such is the case, for example, for α5β1 integrins, whose binding to actin is activated by fibronectin binding, its ligand and by cross-linking (Choquet et al., 1997; Felsenfeld et al., 1996; Kusumi et al., 1993; Saxton and Jacobson, 1997). However, the absence of dependence of the delay for anchoring upon antibody density on the bead renders this hypothesis unlikely. The experimental protocol preferentially initially labels free receptors: beads put in contact with the cell surface initially have a higher probability to bind to diffusive receptors than to stabilized receptors, because the former explore a much larger surface area per unit time. As bead-bound receptors diffuse on the cell surface, after a certain exploration time they can encounter a binding site on a microtubule, or the bead can bind to a new microtubule-bound receptor, and then be transported rearward. The site of anchoring, as well as the movement during the diffusive phase, is on average more proximal to the cell body than the initial point of contact of the bead. This indicates that during diffusion, receptors are already mildly dragged rearward, although this movement is undetectable on individual traces. This could arise, for example, if receptors under the bead accumulate small microtubule fragments that are sensitive to actin flow. The high mobility of receptors in their diffusive state allows for the exploration of large surface areas. This indicates that their presence at the leading edge of lamellipodias does not necessarily involve targeted exocytosis. The Brownian diffusion can also potentially account for the replenishment of receptors removed from the tip of the lamellipodia by rearward movement. Our experiments, however, do not enable the

proportion of receptors being transported at any given moment to be measured.

We have shown microtubule-dependent surface transport of mGluR5. The interaction between mGluR5 and tubulin is not necessarily direct, but could involve intermediates such as microtubule-associated proteins or the associated G_q protein, which has been shown to bind tubulin (Popova et al., 1997). mGluR5 binding to microtubules could be involved in receptor stabilization at given sites, as has been proposed for the glycine receptor (Kirsch et al., 1991). However, in immunocytochemical experiments, we have been unable to detect a colocalization between microtubules and receptors (data not shown). Microtubule-based intracellular vesicular transport of receptors has been shown for ionotropic AMPA (Kim and Lisman, 2001; Setou et al., 2002) and NMDA (Setou et al., 2000) receptors. However, such motor-based transport of receptors along microtubules is much faster (i.e. about 1 μm/s) than the retrograde surface transport we have observed and which is dependent on passive transport of microtubules by the actin flow. Furthermore, we did not observe fast directed transport of receptors on neurites, as would be expected if surface receptors could move on microtubules through binding to a motor protein.

Alternatively, surface transport of mGluRs could help remove or target them to certain cell areas during growth cone migration or cell-cell contact formation. During embryonic development, neurotransmitters such as glutamate may serve as a chemoattractant for growth cones (Zheng et al., 1996). The glutamate gradient is thought to be sensed through NMDA and group I metabotropic receptors as the chemotactic effect of glutamate is abolished in the presence of antagonists of those receptors (Behar et al., 1999). Removal of mGluRs from the leading edge of the growth cone during chemotaxis along a glutamate gradient could help limit the number of receptors as part of an adaptive process. Following this idea, it will be interesting to investigate the role of mGluR5 stimulation on growth cone migration, particularly as glutamate has strong effects on growth cone motility (Zheng et al., 1996). Another attractive hypothesis is that retrograde transport of mGluRs on growth cones is linked to cell-cell contact and synapse formation. We recently showed that cadherins, a family of adhesion proteins essential for synapse formation, are also retrogradely transported on lamellipodias with the actin flux (Lambert et al., 2002). Cadherins and mGluRs are both localized in a perisynaptic annulus around synapses (Lujan et al., 1997; Nusser et al., 1994; Uchida et al., 1996; Vidnyanszky et al., 1994). This peculiar localization could involve their cotransport. Finally, dendritic spines also bear a very active actin cytoskeleton (Matus, 2000). It has been proposed that AMPA receptors may interact first with microtubules during dendritic transport and then with actin during the late phase of targeting, from the dendritic shaft to the spine (Kim and Lisman, 2001). The constant remodeling of actin in the spine could also participate in surface receptor trafficking.

We wish to thank J. P. Pin for the gift of mGluR5 cDNA, O. Thoumine, C. Gardinaru, R. Schmauder and E. Snaar-Jagalska for critical reading of the manuscript, O. Demouy and F. Coussen for assistance in molecular biology, and F. Rossignol and P. Gonzales for cell cultures. This work was supported by grants from the CNRS, the Fondation pour la Recherche Médicale, the Association Française contre les Myopathies, the council of the Région Aquitaine and the European Community grant QLG3-CT-2001-02089.

References

Akaaboune, M., Culican, S. M., Turney, S. G. and Lichtman, J. W. (1999). Rapid and reversible effects of activity on acetylcholine receptor density at the neuromuscular junction in vivo. *Science* **286**, 503-507.

Allison, D. W., Gelfand, V. I., Spector, I. and Craig, A. M. (1998). Role of actin in anchoring postsynaptic receptors in cultured hippocampal neurons: differential attachment of NMDA versus AMPA receptors. *J. Neurosci*. **18**, 2423-2436.

Behar, T. N., Scott, C. A., Greene, C. L., Wen, X., Smith, S. V., Maric, D., Liu, Q. Y., Colton, C. A. and Barker, J. L. (1999). Glutamate acting at NMDA receptors stimulates embryonic cortical neuronal migration. *J. Neurosci.* **19**, 4449-4461.

Borgdorff, A. and Choquet, D. (2002). Regulation of AMPA receptor lateral movement. *Nature* **417**, 649–653.

Choquet, D., Felsenfeld, D. P. and Sheetz, M. P. (1997). Extracellular matrix rigidity causes strengthening of integrin- cytoskeleton linkages. *Cell* **88**, 39-48.

Ciruela, F. and McIlhinney, R. A. (2001). Metabotropic glutamate receptor type 1alpha and tubulin assemble into dynamic interacting complexes. *J. Neurochem.* **76**, 750-757.

Ciruela, F., Robbins, M. J., Willis, A. C. and McIlhinney, R. A. (1999). Interactions of the C terminus of metabotropic glutamate receptor type 1alpha with rat brain proteins: evidence for a direct interaction with tubulin. *J. Neurochem.* **72**, 346-354.

Conn, P. J. and Pin, J.-P. (1997). Pharmacology and functions of metabotropic glutamate receptors. *Annu. Rev. Pharmacol. Toxicol.* **37**, 205-237.

Danuser, G. and Oldenbourg, R. (2000). Probing f-actin flow by tracking shape fluctuations of radial bundles in lamellipodia of motile cells. *Biophys. J.* **79**, 191-201.

Faivre-Sarrailh, C., Falk, J., Pollerberg, E., Schachner, M. and Rougon, G. (1999). NrCAM, cerebellar granule cell receptor for the neuronal adhesion molecule F3, displays an actin-dependent mobility in growth cones. *J. Cell Sci.* **112**, 3015-3027.

Felsenfeld, D. P., Choquet, D. P. and Sheetz, M. P. (1996). Ligand binding regulates the directed movement of b1 integrins on fibroblasts. *Nature* **383**, 438-440.

Grabham, P. W., Foley, M., Umeojiako, A. and Goldberg, D. J. (2000). Nerve growth factor stimulates coupling of beta1 integrin to distinct transport mechanisms in the filopodia of growth cones. *J. Cell Sci.* **113**, 3003-3012.

Hémar, A., Olivo, J.-C., Saffrich, R., Williamson, E. and Dotti, C. G. (1997). Dendroaxonal transcytosis of transferrin in cultured hippocampal and sympathetic neurons. *J. Neurosci.* **17**, 9026-9034.

Kim, C. H. and Lisman, J. E. (2001). A labile component of AMPA receptor-mediated synaptic transmission is dependent on microtubule motors, actin, and N-ethylmaleimide-sensitive factor. *J. Neurosci.* **21**, 4188-4194.

Kirsch, J., Langosch, D., Prior, P., Littauer, U. Z., Schmitt, B. and Betz, H. (1991). The 93-kDa glycine receptor-associated protein binds to tubulin. *J. Biol. Chem.* **266**, 22242-22245.

Kreimborg, K. M., Lester, M. L., Medler, K. F. and Gleason, E. L. (2001). Group I metabotropic glutamate receptors are expressed in the chicken retina and by cultured retinal amacrine cells. *J. Neurochem.* **77**, 452-465.

Kucik, D. F., Elson, E. L. and Sheetz, M. P. (1999). Weak dependence of mobility of membrane protein aggregates on aggregate size supports a viscous model of retardation of diffusion. *Biophys. J.* **76**, 314-322.

Kusumi, A., Sako, Y. and Yamamoto, M. (1993). Confined lateral diffusion of membrane receptors as studied by single particle tracking (nanovid microscopy). Effects of calcium-induced differentiation in cultured epithelial cells. *Biophys. J.* **65**, 2021-2040.

Lambert, M., Choquet, D. and Mege, R. M. (2002). Ligand-induced mobilization of cadherins triggers their anchoring to the actin cytoskeleton through a Rac1-dependent process. *J. Cell Biol.* **157**, 469-479.

Lin, C. H., Espreafico, E. M., Mooseker, M. S. and Forscher, P. (1996). Myosin drives retrograde F-actin flow in neuronal growth cones. *Neuron* **16**, 769-782.

Lujan, R., Roberts, J. D., Shigemoto, R., Ohishi, H. and Somogyi, P. (1997). Differential plasma membrane distribution of metabotropic glutamate receptors mGluR1 alpha, mGluR2 and mGluR5, relative to neurotransmitter release sites. *J. Chem. Neuroanat.* **13**, 219-241.

Mary, S., Gomeza, J., Prezeau, L., Bockaert, J. and Pin, J.-P. (1998). A cluster of basic residues in the carboxyl-terminal tail of the short metabotropic glutamate receptor 1 variants impairs their coupling to phospholipase C. *J. Biol. Chem.* **273**, 425-432.

Matus, A. (2000). Actin-based plasticity in dendritic spines. *Science* **290**, 754-758.

Meier, J., Vannier, C., Sergé, A., Triller, A. and Choquet, D. (2001). Fast and reversible trapping of surface glycine receptors by gephyrin. *Nat. Neurosci.* **4**, 253-260.

Nusser, Z., Mulvihill, E., Streit, P. and Somogyi, P. (1994). Subsynaptic segregation of metabotropic and ionotropic glutamate receptors as revealed by immunogold localization. *Neuroscience* **61**, 421-427.

Pantaloni, D., le Clainche, C. and Carlier, M. F. (2001). Mechanism of actin-based motility. *Science* **292**, 1502-1506.

Passafaro, M., Piech, V. and Sheng, M. (2001). Subunit-specific temporal and spatial patterns of AMPA receptor exocytosis in hippocampal neurons. *Nat. Neurosci.* **4**, 917-926.

Popova, J. S., Garrison, J. C., Rhee, S. G. and Rasenick, M. M. (1997). Tubulin, Gq, and phosphatidylinositol 4,5-bisphosphate interact to regulate phospholipase Cbeta1 signaling. *J. Biol. Chem.* **272**, 6760-6765.

Romano, C., Sesma, M. A., McDonald, C., O'Malley, K., van den Pol, A. and Olney, J. W. (1995). Distribution of metabotropic glutamate receptor mGLuR5 immunoreactivity in rat brain. *J. Comp. Neurol.* **355**, 455-469.

Romano, C., van den Pol, A. N. and O'Malley, K. L. (1996). Enhanced early developmental expression of the metabotropic glutamate receptor mGluR5 in rat brain: protein, mRNA splice variants, and regional distribution. *J. Comp. Neurol.* **367**, 403-412.

Rosenberg, M., Meier, J., Triller, A. and Vannier, C. (2001). Dynamics of glycine receptor insertion in the neuronal plasma membrane. *J. Neurosci.* **21**, 5036-5044.

Saffman, P. G. and Delbruck, M. (1975). Brownian motion in biological membranes. *Proc. Natl. Acad. Sci. USA* **72**, 3111-3113.

Salpeter, M. M. and Loring, R. H. (1985). Nicotinic acetylcholine receptors in vertebrate muscle: properties, distribution and neural control. *Progr. Neurobiol.* **25**, 297-325.

Saxton, M. J. and Jacobson, K. (1997). Single-particle tracking: applications to membrane dynamics. *Annu. Rev. Biophys. Biomol. Struct.* **26**, 373-399.

Schmidt, C. E., Dai, J., Lauffenburger, D. A., Sheetz, M. P. and Horwitz, A. F. (1995). Integrin-cytoskeletal interactions in neuronal growth cones. *J. Neurosci.* 15, 3400-3407.

Sergé, A., Fourgeaud, L., Hémar, A. and Choquet, D. (2002). Receptor activation and homer differentially control the lateral mobility of mGluR5 in the neuronal membrane. *J. Neurosci.* **22**, 3910-3920.

Setou, M., Nakagawa, T., Seog, D. H. and Hirokawa, N. (2000). Kinesin superfamily motor protein KIF17 and mLin-10 in NMDA receptor-containing vesicle transport. *Science* **288**, 1796-1802.

Setou, M., Seog, D. H., Tanaka, Y., Kanai, Y., Takei, Y., Kawagishi, M. and Hirokawa, N. (2002). Glutamate-receptor-interacting protein GRIP1 directly steers kinesin to dendrites. *Nature* **417**, 83-87.

Sheetz, M. P., Turney, S., Qian, H. and Elson, E. L. (1989). Nanometre-level analysis demonstrates that lipid flow does not drive membrane glycoprotein movements. *Nature* **340**, 284-288.

Smith, S. J. (1988). Neuronal cytomechanics: the actin-based motility of growth cones. *Science* **242**, 708-715.

Thompson, C., Lin, C. H. and Forscher, P. (1996). An Aplysia cell adhesion molecule associated with site-directed actin filament assembly in neuronal growth cones [In Process Citation]. *J. Cell Sci.* **109**, 2843-2854.

Tovar, K. R. and Westbrook, G. L. (2002). Mobile NMDA receptors at hippocampal synapses. *Neuron* **34**, 255-264.

Uchida, N., Honjo, Y., Johnson, K. R., Wheelock, M. J. and Takeicji, M. (1996). The catenin/cadherin adhesion system is localized in synaptic junctions bordering translitter release zones. *J. Cell Biol.* **135**, 767-779.

van den Pol, A. N., Obrietan, K., Cao, V. and Trombley, P. Q. (1995). Embryonic hypothalamic expression of functional glutamate receptors. *Neuroscience* **67**, 419-439.

Vidnyanszky, Z., Hamori, J., Negyessy, L., Ruegg, D., Knopfel, T., Kuhn, R. and Gorcs, T. J. (1994). Cellular and subcellular localization of the mGluR5a metabotropic glutamate receptor in rat spinal cord. *NeuroReport* **6**, 209-213.

Waterman-Storer, C. and Salmon, E. (1997). Actomyosin-based retrograde flow of microtubules in the lamella of migrating epithelial cells influences microtubule dynamic instability and turnover and is associated with microtubule breakage and treadmilling. *J. Cell Biol.* **139**, 417-434.

Zheng, J. Q., Wan, J. J. and Poo, M. M. (1996). Essential role of filopodia in chemotropic turning of nerve growth cone induced by a glutamate gradient. *J. Neurosci.* **16**, 1140-1149.

Zhou, Q., Xiao, M. and Nicoll, R. A. (2001). Contribution of cytoskeleton to the internalization of AMPA receptors. *Proc. Natl. Acad. Sci. USA* **98**, 1261-1266.